Journal of Luminescence 145 (2014) 38–48

Contents lists available at ScienceDirect

Journal of Luminescence

journal homepage: www.elsevier.com/locate/jlumin

Thermal dependence of luminescence lifetimes and radioluminescence in quartz

V. Pagonis [a,*], M.L. Chithambo [b], R. Chen [c], A. Chruścińska [d], M. Fasoli [e], S.H. Li [f], M. Martini [e], K. Ramseyer [g]

[a] McDaniel College, Physics Department, Westminster, MD 21157, USA
[b] Department of Physics and Electronics, Rhodes University, PO BOX 94, Grahamstown 6140, South Africa
[c] Raymond and Beverly Sackler School of Physics and Astronomy, Tel-Aviv University, Tel-Aviv 69978, Israel
[d] Institute of Physics, Nicholas Copernicus University, 87-100 Toruń, Poland
[e] Department of Materials Science, University of Milano-Bicocca, Via Cozzi 53, 20125 Milano, Italy
[f] Department of Earth Sciences, The University of Hong Kong, Hong Kong
[g] Institut für Geologie, Baltzerstrasse 1+3, 3012 Bern, Switzerland

ARTICLE INFO

Article history:
Received 8 March 2013
Received in revised form
1 July 2013
Accepted 10 July 2013
Available online 18 July 2013

Keywords:
Time resolved luminescence
Pulsed luminescence
Quartz luminescence lifetimes
Thermal quenching
Kinetic model
Radioluminescence

ABSTRACT

During time-resolved optical stimulation experiments (TR-OSL), one uses short light pulses to separate the stimulation and emission of luminescence in time. Experimental TR-OSL results show that the luminescence lifetime in quartz of sedimentary origin is independent of annealing temperature below 500 °C, but decreases monotonically thereafter. These results have been interpreted previously empirically on the basis of the existence of two separate luminescence centers L_H and L_L in quartz, each with its own distinct luminescence lifetime. Additional experimental evidence also supports the presence of a non-luminescent hole reservoir *R*, which plays a critical role in the predose effect in this material. This paper extends a recently published analytical model for thermal quenching in quartz, to include the two luminescence centers L_H and L_L, as well as the hole reservoir *R*. The new extended model involves localized electronic transitions between energy states *within* the two luminescence centers, and is described by a system of differential equations based on the Mott–Seitz mechanism of thermal quenching. It is shown that by using simplifying physical assumptions, one can obtain analytical solutions for the intensity of the light during a TR-OSL experiment carried out with previously annealed samples. These analytical expressions are found to be in good agreement with the numerical solutions of the equations. The results from the model are shown to be in quantitative agreement with published experimental data for commercially available quartz samples. Specifically the model describes the variation of the luminescence lifetimes with (a) annealing temperatures between room temperature and 900 °C, and (b) with stimulation temperatures between 20 and 200 °C. This paper also reports new radioluminescence (RL) measurements carried out using the same commercially available quartz samples. Gaussian deconvolution of the RL emission spectra was carried out using a total of seven emission bands between 1.5 and 4.5 eV, and the behavior of these bands was examined as a function of the annealing temperature. An emission band at ~3.44 eV (360 nm) was found to be strongly enhanced when the annealing temperature was increased to 500 °C, and this band underwent a significant reduction in intensity with further increase in temperature. Furthermore, a new emission band at ~3.73 eV (330 nm) became apparent for annealing temperatures in the range 600–700 °C. These new experimental results are discussed within the context of the model presented in this paper.

1. Introduction

The experimental technique of time-resolved optically stimulated luminescence (TR-OSL) is an important tool for studying luminescence mechanisms in a variety of materials, and finds extensive applications in the field of luminescence dosimetry and luminescence dating [1–8]. While continuous-wave optically stimulated luminescence (CW-OSL) measurements are more common in quartz applications, TR-OSL is a valuable probe in the study of recombination and/or relaxation pathways in the material.

During TR-OSL measurements the stimulation is carried out with a brief light pulse, and the signals from several pulses are summed to obtain a typical TR-OSL curve consisting of a buildup of

* Corresponding author. Tel.: +1 410 857 2481; fax: +1 410 386 4624.
E-mail address: vpagonis@mcdaniel.edu (V. Pagonis).

0022-2313/$ - see front matter © 2013 Elsevier B.V. All rights reserved.
http://dx.doi.org/10.1016/j.jlumin.2013.07.022

the signal during the pulse, followed by the subsequent decrease when the optical stimulation is turned off. The decaying part of the luminescence signal is usually analyzed with a linear sum of exponential decays, and is characterized by the corresponding luminescence lifetimes. Several researchers have studied the temperature dependence of luminescence lifetimes and luminescence intensity from time-resolved luminescence experiments in quartz (see for example, [9–13] and references therein). Luminescence lifetimes for unannealed quartz of sedimentary origin (for convenience hereafter referred to as sedimentary quartz) are typically found to remain constant at ~42 μs for stimulation temperatures between 20 °C and 100 °C, and then to decrease continuously to ~8 μs at a stimulation temperature of 200 °C. This decrease of the luminescence lifetime with stimulation temperature is usually described within the framework of the well-known phenomenon of thermal quenching of luminescence in quartz. Thermal quenching has also been observed in both thermoluminescence (TL) and CW-OSL experiments on quartz [14,15], and is commonly described using the Mott–Seitz mechanism (see for example [16–18] and references therein).

Several experimental studies have shown that time resolved luminescence from sedimentary quartz annealed below 500 °C is dominated by a single exponential component, with a luminescence lifetime τ_H~42 μs, which is independent of irradiation dose [10–13,19]. However, when sedimentary quartz samples are annealed at temperatures above 500 °C, one observes that the effective luminescence lifetime decreases continuously thereafter to a characteristic value of τ_L~32–35 μs [9,11,20–22]. These results have been interpreted previously empirically by proposing the existence of two separate luminescence centers L_H and L_L in quartz, each with its own distinct luminescence lifetime τ_H and τ_L correspondingly. In addition, the existence of a non-luminescent hole reservoir R has been proposed, on the basis of the predose effect exhibited by this material. The predose effect is usually interpreted empirically on the basis of thermal transfer of holes taking place between the distinct luminescence centers in quartz.

Recently Pagonis et al. [20] presented a new kinetic model for thermal quenching in quartz which is based on the Mott–Seitz mechanism. In this model all recombination transitions are localized within the recombination center (in contrast to delocalized models in which all charge transitions take place via the conduction and valence bands [18]). In later work Pagonis et al. [21] developed analytical expressions for the luminescence intensity observed during and after the short pulses used during a TR-OSL experiment. These analytical expressions were derived by assuming that the traps are well below saturation, and were compared with the numerical solutions of the system of differential equations.

The specific goals of the present paper are

(a) To expand the recently published quartz model of Pagonis et al. [20,21], in an effort to include the experimentally observed lifetimes τ_H and τ_L for sedimentary quartz samples.
(b) To describe mathematically the experimentally observed decrease of the luminescence lifetime from a value of τ_H~42 μs for unannealed sedimentary quartz samples, to a value of τ_L~32 μs for samples annealed above 500°C.
(c) To describe mathematically the experimentally observed decrease of the luminescence lifetime with the stimulation temperature used during a TR-OSL experiment.
(d) To carry out a quantitative comparison of the modeled results from parts (b) and (c) above, with published experimental data for a commercially available quartz sample.
(e) To supplement the published TR-OSL data with new radioluminescence (RL) data obtained using the *same* commercial quartz samples, after annealing at elevated temperatures.

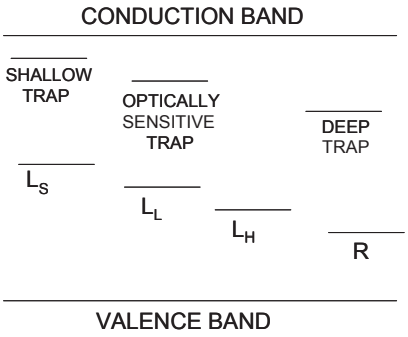

Fig. 1. A model for luminescence lifetimes in quartz from Ref. [9], showing the 3 radiative luminescence centers denoted by L_H, L_L and L_S and the non-radiative luminescence center R. Centers L_H, L_L and R are dominant in sedimentary quartz.

2. Luminescence lifetimes in quartz: the T_H, T_L and T_S components

This section presents an overview of experimentally observed luminescence lifetimes in quartz samples. Fig. 1 shows a simple energy scheme model which has been proposed based on extensive experimental studies of luminescence lifetimes in quartz (see for example Galloway [9]; Chithambo and Galloway [19]; Chithambo and Ogundare [22]). The energy scheme in Fig. 1 consists of three independent radiative luminescence centers denoted by L_H, L_L and L_S, and a non-radiative luminescence center denoted by R. These radiative centers are associated with distinct characteristic lifetimes denoted by τ_H, τ_L and τ_S correspondingly (Galloway [9]). It is also assumed that all three luminescence centers contribute to the experimentally observed optically stimulated luminescence and that the experimentally observed lifetime will depend on which of the three centers is dominant.

According to this energy scheme, time resolved luminescence from sedimentary quartz annealed below 500 °C is dominated by a single component with a luminescence lifetime τ_H ~42 μs [9–13]. It is believed that high temperature annealing of quartz samples above ~500°C causes the redistribution of holes between the non-radiative center R and the three radiative centers denoted by L_H, L_L and L_S. As a result of this redistribution of holes, luminescence from centers other than L_H becomes more important.

In the rest of this paper, the discussion and model will concern sedimentary quartz samples, and will therefore refer only to luminescence centers L_H, L_L and their distinct characteristic lifetimes τ_H, τ_L correspondingly. In addition, the non-radiative hole center R will also be discussed in the context of the model.

3. The new model

This section summarizes the main points of the recent model of Pagonis et al. [20,21], and the model is extended to the case of two luminescence centers. The physical basis of explaining thermal quenching within the model is based on the Mott–Seitz mechanism. The model involves electronic transitions between energy states *within* the recombination center. The original model of Pagonis et al. [21] is shown in Fig. 2. Fig. 2a shows the configurational diagram for thermal quenching processes based on the Mott–Seitz mechanism, while Fig. 2b shows the proposed electronic transitions taking place within the model.

In this paper we extend the model shown in Fig. 2a, to include the two independent luminescence centers L_H and L_L, as well as the non-radiative hole reservoir R. Fig. 3 shows the new extended model, which is also based on the Mott–Seitz mechanism. The arrows in Fig. 3 indicate the electronic transitions which are likely

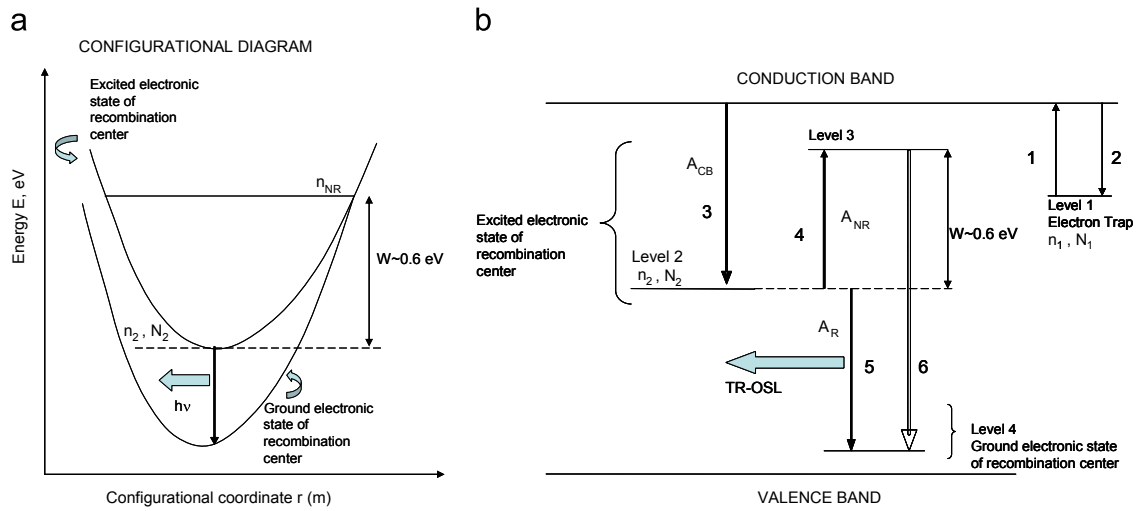

Fig. 2. The model of Pagonis et al. [20,21] for thermal quenching in quartz, based on the Mott–Seitz mechanism. (a) The configurational coordinate diagram for thermal quenching processes and (b) the electronic transitions taking place within the model. The various parameters are discussed in the text.

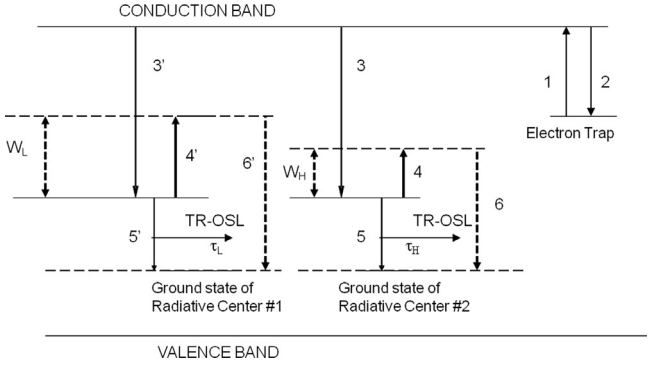

Fig. 3. Schematic representation of the model proposed in this paper to explain the luminescence lifetimes for annealed quartz samples. The model of Fig. 2b is extended for the case of two luminescence centers L_H and L_L, each with its own distinct luminescence lifetime. In transition 1 electrons from a dosimetric trap are raised by optical stimulation into the CB, with some of these electrons being retrapped as shown in transition 2 with a probability A_n. Transitions 3 and 3′ correspond to electronic transitions from the CB into the excited states located below the conduction band, with probability A_{CB}. Transitions 5 and 5′ indicate the direct *radiative* transition from the excited levels into the ground electronic states for L_H and L_L, with probabilities $(A_R)_H$ and $(A_R)_L$and transitions 4 and 4′ indicate the competing thermally assisted routes. Transitions 6 and 6′ denote the non-radiative processes into the ground state. Thermal quenching is caused by the competing transitions 4, 5 within luminescence center L_H and 4′, 5′ within center L_L.

to be taking place during a typical TR-OSL experiment. The simplified model consists of a dosimetric trap, and several levels representing energy states within the two distinct recombination centers L_H and L_L. During the transition labeled 1, electrons from a dosimetric trap are raised by optical stimulation into the CB, with some of these electrons being retrapped as shown in transition 2 with a probability A_n. Several additional transitions labeled 3–6 and 3′–6′ are shown in Fig. 3, corresponding to these two luminescence centers respectively.

Transitions 3 and 3′ correspond to electronic transitions from the CB into the excited states located below the conduction band, with probability A_{CB}. Transitions 5 and 5′ indicate the direct *radiative* transition from the excited levels into the ground electronic states for L_H and L_L, with probabilities $(A_R)_H$ and $(A_R)_L$correspondingly. Transitions 4 and 4′ indicate the competing thermally assisted routes respectively. The probabilities for these competing thermally assisted processes are given by Boltzmann factors of the form $(A_{NR})_H \exp(-W_H/k_BT)$, and $(A_{NR})_L \exp(-W_L/k_BT)$. Here W_H and W_L represent the activation energy for these processes and $(A_{NR})_H$, $(A_{NR})_L$ are constants representing the non-radiative transition probabilities. Transitions 6 and 6′ denote the non-radiative processes into the ground state. As discussed in Pagonis et al. [20], the details of the non-radiative process in the model are not important for the purposes of this model.

Thermal quenching within this model is caused by the competing transitions 4, 5 within luminescence center L_H and 4′, 5′ within center L_L in Fig. 3, correspondingly. As the temperature of the sample is increased, electrons are removed from the excited states according to the Boltzmann factors described above. This reduction leads to both a decrease of the intensity of the luminescence signal and to a simultaneous decrease of the two apparent luminescence lifetimes τ_H and τ_L.

The notation and parameters used in the model of this paper are similar to those used in Pagonis et al. [20], and are defined as follows. N_1 is the concentration of the dosimetric electron traps (cm^{-3}), n_1 is the corresponding concentration of trapped electrons (cm^{-3}). N_H, N_L (cm^{-3}) are the total concentrations of luminescence centers and N_H–n_H, N_L–n_L are the corresponding concentrations of activated luminescence centers (cm^{-3}) respectively. A detailed discussion of the connection between the concentrations N_H, N_L, N_H–n_H, N_L–n_L and the concentrations of specific defects in quartz can be found in ([21], p. 1835). Electrons trapped in each of these states can undergo either a radiative transition into the ground state, or a competing non-radiative transition.

A_{CB} is the probability coefficient ($cm^3\ s^{-1}$) for transitions taking place from the conduction band into the two excited states. For simplicity, it is assumed that electrons can be captured from the CB into the excited states of L_H and L_L with the same capture probability A_{CB}. The function n_c represents the instantaneous concentration of electrons in the conduction band (cm^{-3}) and P denotes the probability of optical excitation of electrons from the dosimetric trap (s^{-1}). The two radiative transitions are characterized by transition probabilities $(A_R)_H, (A_R)_L$ which are related to the quartz luminescence lifetimes τ_H, τ_L by the expressions $(A_R)_H = 1/\tau_H$ and $(A_R)_L = 1/\tau_L$.

The equations in the model are

$$\frac{dn_1}{dt} = n_c(N_1 - n_1)A_n - n_1 P \tag{1}$$

$$\frac{dn_c}{dt} = -n_c(N_1 - n_1)A_n + n_1 P - A_{CB} n_c(N_H - n_H) - A_{CB} n_c(N_L - n_L) \tag{2}$$

$$\frac{dn_H}{dt} = A_{CB}n_c(N_H - n_H) - (A_R)_H n_H - n_H(A_{NR})_H \exp(-W_H/k_BT) \quad (3)$$

$$\frac{dn_L}{dt} = A_{CB}n_c(N_L - n_L) - (A_R)_L n_L - n_L(A_{NR})_L \exp(-W_L/k_BT) \quad (4)$$

The total instantaneous luminescence $I(t)$ resulting from the two radiative transitions is defined as

$$I(t) = (A_R)_H n_H + (A_R)_L n_L. \quad (5)$$

As in the previous simpler version of the model [20,21], it is assumed that during a TR-OSL pulse the concentration of electrons in the dosimetric trap $n_1(t)$ does not change appreciably, and that the electronic levels n_L and n_H are away from saturation, i.e. $n_1 \approx n_1(0), n_H \ll N_H$ and $n_L \ll N_L$. Here $n_1(0)$represents the initial concentration of trapped electrons in the dosimetric trap. Under these conditions, Eq. (2) can be written as

$$\frac{dn_c}{dt} = -n_c(N_1 - n_1(0))A_n + n_1(0)P - A_{CB}n_c N_H - A_{CB}n_c N_L. \quad (6)$$

This first order differential equation can be integrated to yield a saturating exponential function

$$n_c = \frac{n_1(0)P}{A_n(N_1 - n_1(0)) + A_{CB}(N_H + N_L)}(1 - \exp\{-[A_n(N_1 - n_1(0)) + A_{CB}(N_H + N_L)]t\}) \quad (7)$$

As discussed previously in [21], this equation informs that after a short time of the order of ~1 μs, the concentration of electrons in the CB reaches a constant quasistatic value given by

$$n_c = \frac{n_1(0)P}{A_n(N_1 - n_1(0)) + A_{CB}(N_H + N_L)}. \quad (8)$$

By substituting this quasistatic value of n_c into Eq. (3) and using $n_H \ll N_H$, yields

$$\frac{dn_H}{dt} = A_{CB}\frac{n_1(0)P}{A_n(N_1 - n_1(0)) + A_{CB}(N_H + N_L)}N_H - (A_R)_H n_H - n_H(A_{NR})_H \exp(-W_H/k_BT) \quad (9)$$

or by setting the constant

$$g = \frac{A_{CB}n_1(0)P}{A_n(N_1 - n_1(0)) + A_{CB}(N_H + N_L)} \quad (10)$$

one obtains from Eq. (9):

$$\frac{dn_H}{dt} = gN_H - n_H\left[(A_R)_H + (A_{NR})_H \exp(-W_H/k_BT)\right]. \quad (11)$$

The solution of this differential equation during the light stimulation period from $t=0$ to $t=t_o$ is given by a saturating exponential of the form

$$n_H(t) = gN_H\frac{1}{(A_R)_H + (A_{NR})_H \exp(-W_H/k_BT)}(1 - \exp\{-\left[(A_R)_H + (A_{NR})_H \exp(-W_H/k_BT)\right]t\}) \quad (12)$$

or

$$n_H(t) = \frac{gN_H}{\gamma_H}(1 - e^{-\gamma_H t}), \quad \text{for } 0 \le t \le t_o \quad (13)$$

where we have set the constant γ_H as

$$\gamma_H = (A_R)_H + (A_{NR})_H \exp(-W_H/kT). \quad (14)$$

The corresponding solution $n_H(t)$ when the optical stimulation is turned OFF, is a simple exponential of the form

$$n_H(t) = n_H(t_o)e^{-\gamma_H(t - t_o)}, \quad \text{for } t \ge t_o \quad (15)$$

where $n_H(t_o)$ is the concentration at the end of the optical stimulation period t_o.

Eqs. (13) and (15) in this paper are the exact analog of the previously derived expressions (14) and (16) in the simpler model of Pagonis et al. [21].

In a similar manner, one arrives at the corresponding symmetric expression for the concentration of electrons n_L in the second luminescence center L_L while the optical stimulation is ON

$$n_L(t) = \frac{gN_L}{\gamma_L}(1 - e^{-\gamma_L t}), \quad \text{for } 0 \le t \le t_o \quad (16)$$

where the constant γ_L is defined as

$$\gamma_L = (A_R)_L + (A_{NR})_L \exp(-W_L/kT). \quad (17)$$

The concentration $n_L(t)$ when the optical stimulation is turned OFF is also a simple exponential of the form

$$n_L(t) = n_L(t_o)e^{-\gamma_L(t - t_o)} \quad \text{for } t \ge t_o. \quad (18)$$

The luminescence intensity $I(t)$ when the LEDs are ON, is obtained by inserting Eqs. (13) and (16) into Eq. (5)

$$I_{ON}(t) = (A_R)_H n_H + (A_R)_L n_L = \frac{(A_R)_H gN_H}{\gamma_H}(1 - e^{-\gamma_H t}) + \frac{(A_R)_L gN_L}{\gamma_L}\left[1 - e^{-\gamma_L t}\right] \quad 0 \le t \le t_o \quad (19)$$

It is noted that the factor g in this equation depends also on the concentrations N_H and N_L.

Similarly we obtain the luminescence intensity when the optical stimulation is OFF

$$I_{OFF}(t) = (A_R)_H n_H + (A_R)_L n_L = (A_R)_H n_H(t_o)e^{-\gamma_H(t - t_o)} + (A_R)_L n_L(t_o)e^{-\gamma_L(t - t_o)} \quad t \ge t_o \quad (20)$$

Eqs. (19) and (20) express the luminescence intensity as a function of the stimulation temperature T and as a function of optical stimulation time t. It is noted that the factor g in Eqs. (10) and (19) contain information on the properties of the dosimetric trap. The factors γ_H and γ_L contain the kinetic parameters of the thermal quenching process, and the stimulation temperature T. As discussed in the next section, the total concentrations N_H and N_L depend on whether the quartz sample has undergone a high temperature annealing or not. The effect of high temperature annealing is expressed in mathematical form in the next section.

4. The effect of high temperature annealing on N_L

According to the empirical energy scheme of Fig. 1, annealing of the sample before measurement causes a redistribution of holes among the recombination centers L_H, L_L. In the case of sedimentary quartz, the experimentally observed luminescence is believed to originate exclusively at recombination centers L_H, L_L. At room temperature, the concentration N_H is greatest, and the apparent dominant experimental luminescence lifetime will correspond to τ_H. At higher annealing temperatures, it is hypothesized that the concentration N_L will increase, and the luminescence lifetime τ_L will become progressively dominant at these higher annealing temperatures. The increase of N_L is believed to take place due to a thermal transfer of holes, possibly taking place via the valence band. It has also been suggested that these thermally transferred holes possibly originate from thermal decomposition of the non-luminescent recombination center R [9].

According to this energy scheme, in *unannealed* sedimentary quartz samples there are many more active luminescence centers in L_H than in L_L. Mathematically this can be expressed as $N_H \gg N_L$. Examination of Eq. (19) with $N_H \gg N_L$ shows that the first term in this equation will become much larger that the second term, and therefore luminescence from L_H will be the dominant term. This means that experimentally one would measure a luminescence lifetime of τ_H~42 μs for unannealed sedimentary quartz samples.

Conversely, for samples annealed above 500 °C, the reverse condition $N_H \ll N_L$ will be true, and the second term in Eq. (19) will be much larger that the first term. In this case luminescence from L_L will be the dominant term, and one would measure a luminescence lifetime of $\tau_L \sim 35$ μs for samples annealed above 500 °C.

The following discussion is based on the following physical assumptions:

(a) It is assumed that the concentration of centers N_H is constant and independent of the annealing temperature.
(b) By contrast, the concentration of centersN_L is assumed to depend strongly on the annealing temperature.
(c) The non-radiative recombination center R in Fig. 1 becomes thermally unstable as the annealing temperature is increased above 500 °C. Holes are assumed to be thermally released from the hole reservoir R, and these are subsequently captured preferentially into L_L, possibly via the valence band. This process of thermal release of holes and their subsequent capture at the luminescent center has been proposed to explain the predose effect in quartz, and has been simulated previously using kinetic models ([17], p. 261).

In order to describe the variation of the luminescence lifetime with the annealing temperature, one must express mathematically the quantity N_L in Eq. (19), as a function of the annealing temperature T_{anneal}.

In general terms, thermal stability of the hole reservoir R will be characterized by a thermal activation energy E_R and a corresponding frequency factor s_R. We further assume first order kinetics for the thermal properties of R. Under this assumption, if the quartz sample is annealed at a temperature T_{anneal} for a time period t_{anneal}, the instantaneous concentration $N_R(t)$ will vary according to the first order decay exponential

$$N_R(t_{anneal}) = N_R(0)\exp(-\lambda t_{anneal}) \tag{21}$$

where $N_R(0)$ represents the initial concentration (i.e. the concentration of holes in R for unannealed samples). The decay constant λ for a first order process is related to the activation energy E_R and the frequency factor s_R by the expression (Chen and Pagonis, [17])

$$\lambda = s_R \exp(-E_R/kT) \tag{22}$$

In this expression the temperature T represents the anneal temperature, T_{anneal}. By combining the last two equations, the instantaneous concentration of centers of type N_R will vary according to

$$N_R(T_{anneal}, t_{anneal}) = N_R(0)\exp[-s_R \exp(-E_R/kT_{anneal})t_{anneal}] \tag{23}$$

or

$$N_R(T_{anneal}) = N_R(0)\exp[-B\exp(-E_R/kT_{anneal})] \tag{24}$$

where the dimensionless constant $B = s_R t_{anneal}$ depends on the amount of time t_{anneal} the sample is kept at the annealing temperature T_{anneal}, and on the frequency s_R of the thermal activation process. In this paper the constant B is treated as a parameter which can be adjusted to fit the experimental data. It is likely that the thermal activation process for hole reservoir R is ionic in nature and it has been characterized previously experimentally by a thermal activation energy $E_W \sim 1.4$ eV [9].

Eq. (24) expresses the concentration of holes *remaining* at the non-radiative center R in Fig. 1, as a function of the annealing temperature. The total concentration of thermally *released* holes $N_{released}$will be given by the difference between the initial and remaining concentrations of holes in R, namely

$$N_{released}(T_{anneal}) = N_R(0) - N_R(0)\exp\left[-B\exp(-E_R/kT_{anneal})\right] \tag{25}$$

According to the proposed energy scheme, these holes are preferentially captured in L_L and therefore the concentration N_L will increase by the same amount according to

$$N_L(T_{anneal}) = N_L + N_{released}(T_{anneal}) = N_L + N_R(0) - N_R(0)\exp[-B\exp(-E_R/kT_{anneal})] \tag{26}$$

or

$$N_L(T_{anneal}) = N_L + N_R(0)\left(1-\exp[-B\exp(-E_R/kT_{anneal})]\right) \tag{27}$$

where N_L denotes the constant concentration of holes in L_L for *unannealed* samples. This is the desired equation, expressing the variation of holes in L_L as a function of the annealing temperature. Typical graphs of the functions in Eqs. (24) and (27) as a function of the annealing temperature are shown in Fig. 4. As the annealing temperature increases, the concentration $N_L(T_{anneal})$ also increases and reaches a maximum at an annealing temperature of ~700 °C, when all holes have been thermally released from R and captured in L_L.

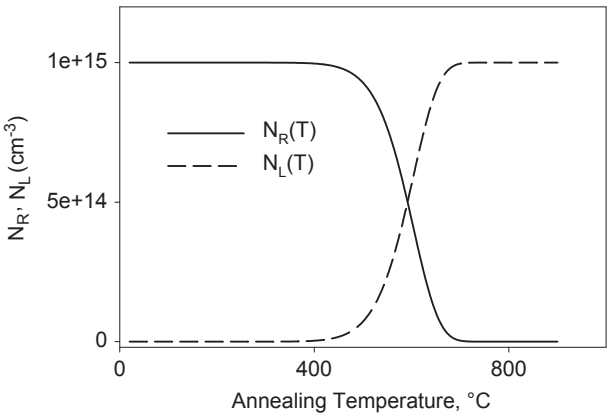

Fig. 4. Simulated thermal transfer of holes as a function of the annealing temperature, based on Eqs. (24) and (27) discussed in the text. As the annealing temperature increases, holes are thermally released from R and captured in L_L. As a consequence, the concentration N_L increases and reaches a maximum at ~700°C, when the thermal transfer process is complete.

By combining Eqs. (10), (19), (20) and (27) one arrives at the desired equations which express the TR-OSL intensity as a function of the stimulation temperature T, and for various annealing temperatures T_{anneal}. The luminescence intensity when the optical stimulation is ON and OFF is given respectively by the following equations:

$$I_{ON}(t) = \frac{A_{CB} n_1(0) P}{A_n(N_1 - n_1(0)) + A_{CB}[N_H + N_L(T_{anneal})]}\left[\frac{(A_R)_H N_H}{\gamma_H}(1-e^{-\gamma_H t}) + \frac{(A_R)_L N_L(T_{anneal})}{\gamma_L}\left[1-e^{-\gamma_L t}\right]\right] \tag{28}$$

(during the pulse),

$$I_{OFF}(t) = n_H(t_o)e^{-\gamma_H(t-t_o)} + n_L(t_o)e^{-\gamma_L(t-t_o)} \tag{29}$$

(after the pulse).

It is noted that the quantities $\gamma_H$and $\gamma_L$in Eq. (28) depend on the stimulation temperature T used during the TR-OSL experiment, while the quantity $N_L(T_{anneal})$ depends on the annealing temperature T_{anneal} according to Eq. (27). Hence Eqs. (28) and (29) contain the dependence of the luminescence signal on both the stimulation temperature T and on the annealing temperature T_{anneal}.

In the next section, the results from these analytical equations are compared with available experimental data from the literature.

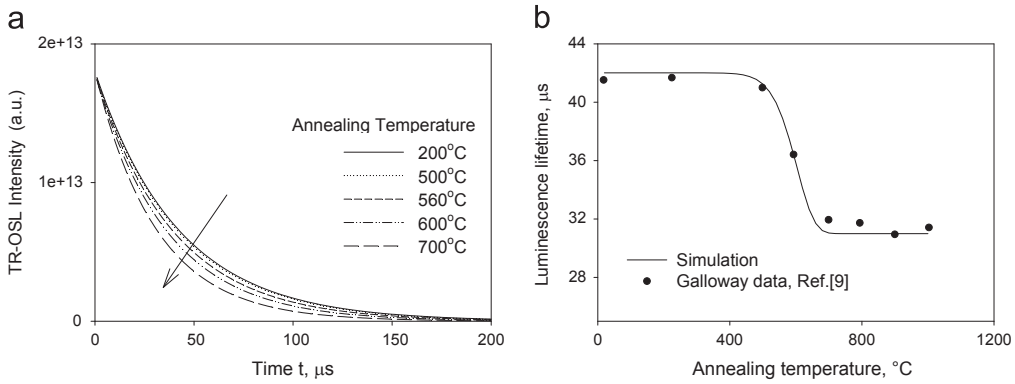

Fig. 5. (a) Simulated TR-OSL intensity measured *at room temperature*, obtained by solving the system of differential equations in the model. Several results are shown, obtained using different annealing temperatures T_{anneal} in the simulations. The same curves are also obtained from the analytical Eqs. (28) and (29). (b)The luminescence lifetimes obtained by fitting a single exponential function to the data in (a) are shown as a continuous line. These are compared with the experimental data shown as solid circles in Fig. 4 of Ref. [9].

5. Numerical and simulated results: single exponential analysis of modeled luminescence signals

In this section the results from the model are compared with examples of experimental data available for commercially available quartz samples (BDH Ltd., UK). These samples consist of 'acid-washed' sand of size 90–500 μm and their luminescence behavior has been studied previously rather extensively [9–13,19,22]. Figs. 5 and 6 show the results of comparing the experimental data from ([9] Figs. 4, 10 and 11), with the analytical equations presented in the previous section.

The numerical values chosen for the parameters in the model were as follows: $A_n = 5 \times 10^{-14}$ cm^{3}s^{-1}, $A_{CB} = 10^{-8}$ cm^{3}s^{-1}, $P = 0.2$ s^{-1}, $N_1 = 10^{14}$ cm^{-3}, $N_H = 10^{14}$ cm^{-3}, $N_L = 10^{13}$ cm^{-3}, and $N_R(0) = 10^{15}$ cm^{-3} at room temperature. The value of $N_H = 10^{14}$ cm^{-3} is chosen to be ten times larger than the value of $N_L = 10^{13}$ cm^{-3}, so that the luminescence center L_H is dominant for unannealed samples. Also the total concentration of holes $N_R(0) = 10^{15}$ cm^{-3} in the hole reservoir R for unannealed samples is chosen a few orders of magnitude larger than the values of N_H andN_L, so that the hole transfer process will cause L_L to become the dominant center at high annealing temperatures. The values of the radiative transition probabilities $(A_R)_H = 1/42\ \mu s = 2.38 \times 10^4$ s^{-1} and $(A_R)_L = 1/32\ \mu s = 3.12 \times 10^4$ s^{-1} are estimated from experimental luminescence lifetimes at room temperature. The initial conditions for the different concentrations at time $t=0$ are taken as $n_1(0) = 9 \times 10^{13}$ cm^{-3}, $n_H(0) = 0$, $n_L(0) = 0$, $n_c(0) = 0$. The thermal quenching parameters are taken as $W_H = W_L = 0.74$ eV, $C = 1.3 \times 10^{13}$ s^{-1}, $E_R = 1.4$ eV from the experimental work in Ref. [9]. It was found that an empirical value of $B = 10^8$ in Eq. (27) produces a good fit to the available experimental data from Ref. [9]. It is noted that the constant $B = st_{anneal}$ in Eq. (27) depends on the annealing time, and hence is an important experimentally controlled parameter. As usual in this type of model, the absolute values of the defect concentrations are not critical, but rather it is their relative concentrations between them that determine the behavior of the model. For example, in the case of natural quartz it is estimated that the actual concentrations would be approximately 1000 times larger than the values of the concentrations used in this paper.

In Fig. 5(a) we show the simulated TR-OSL intensity measured *at room temperature*, obtained by solving the system - of differential equations in the model for different annealing temperatures. Alternatively, these same curves can be obtained from the analytical Eqs. (28) and (29). The analytical and numerical solutions were found to be identical, within an accuracy of 1% or better.

Fig. 5(b) shows the luminescence lifetimes obtained by fitting a single exponential function to the data of Fig. 5(a); the simulated data (continuous line) are compared with the experimental data shown as solid circles in Fig. 4 of Galloway [9]. It is concluded that the model presented in this paper provides a satisfactory mathematical description of the experimentally observed transition from the luminescence lifetime of τ_H at low annealing temperatures $T_{anneal} < 500$ °C, to a value of τ_L at high annealing temperatures, as shown in Fig. 5(b).

The change in lifetime with annealing temperature from the higher value τ_H to the lower luminescence lifetime τ_L has also been described previously by the empirical expression [9]

$$\tau(T) = \tau_L + \frac{(\tau_H - \tau_L)}{1 + C\,\exp(-E_W/kT)} \tag{28}$$

where C is a dimensionless constant, k is the Boltzmann constant, T is the annealing temperature and $E_W = 1.4$ eV is the thermal activation energy for the thermal transfer of holes into L_L (see Ref. [9], legend of their Fig. 4). This empirical expression is also in close agreement with the experimental data shown in Fig. 5(b).

Fig. 6 shows the modeled luminescence lifetimes and the corresponding normalized intensities as a function of the stimulation temperature T used during the TR-OSL process. In Fig. 6 the simulated luminescence lifetimes and intensities from this paper are shown as continuous lines, for three quartz samples which were previously annealed at 20, 500 and 800 °C. These simulated solid lines are compared with the experimental data taken from Figs. 10 and 11 of Ref. [9].

The solid circles in Fig. 6(a) through (d) indicate the results obtained in Ref. [9] by fitting the experimental data with a single exponential component. The solid circles and open squares in Fig. 6(e)–(f) indicate the results obtained in Ref. [9] by fitting the experimental data with two exponential components. All intensity results shown here were normalized to the initial value at room temperature. Fig. 6(e)–(f) show significant differences between the model and the experimental data for the sample annealed at 800 °C. In practice, Chithambo and Ogundare [22] found that the number of lifetimes that can be evaluated from a TR-OSL signal depends on the combination of annealing and measurement temperature used in the experiment. For quartz annealed up to 500 °C, only one lifetime is found and this is independent of irradiation dose, whereas for higher annealing temperatures multiple lifetimes are usually found for very high irradiation doses [9,22].

It is also noted that the experimental data in Fig. 6(e)–(f) shows an initial increase of the luminescence intensity and luminescence lifetime at low stimulation temperatures. This is a well known experimental result which has been reported in several materials.

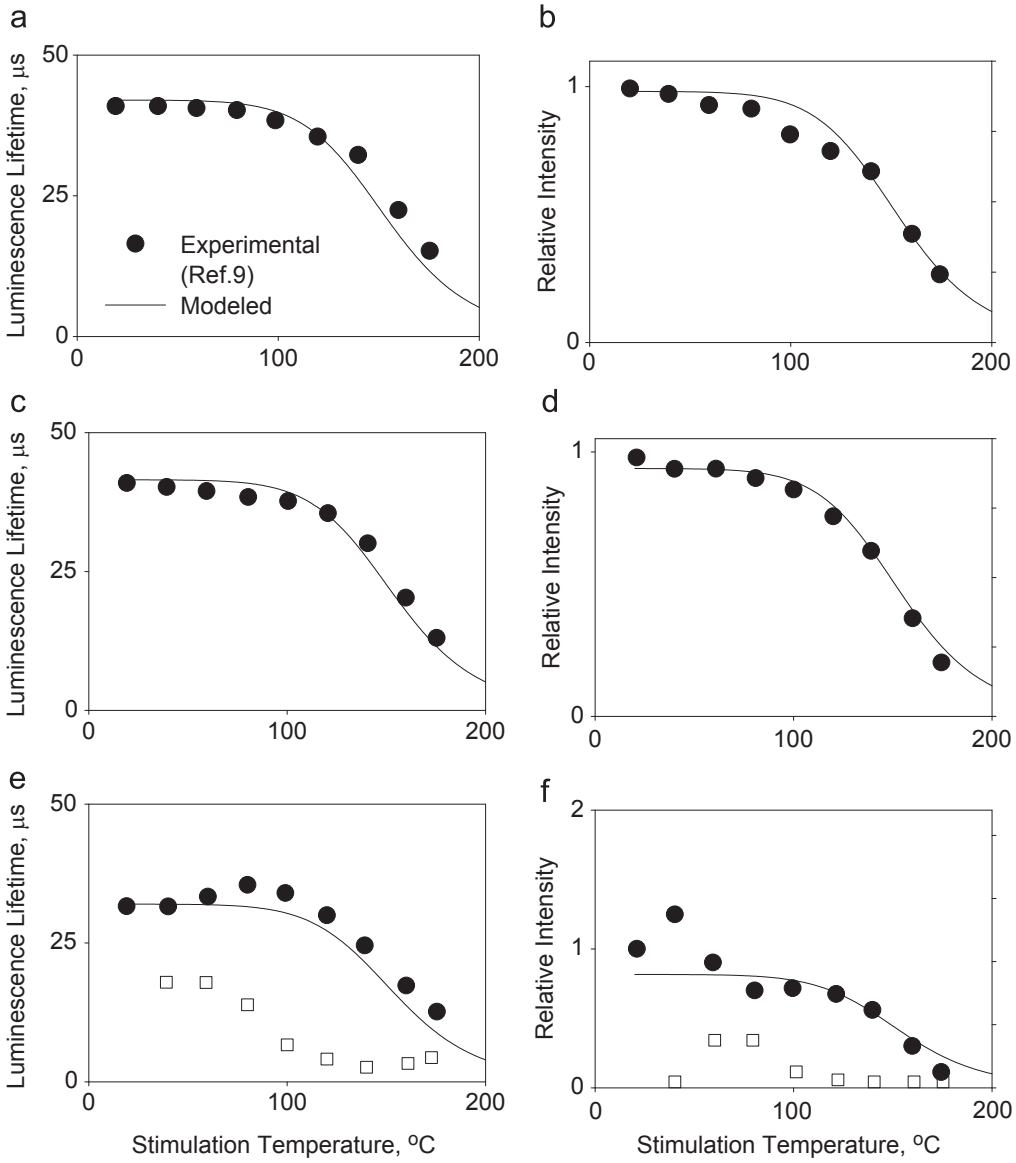

Fig. 6. Comparison of the modeled and experimental luminescence lifetimes and luminescence intensities, as a function of the stimulation temperature used during the TR-OSL process. Several examples are shown, for samples previously annealed at 20 °C (a)–(b), 500 °C (c)–(d) and 800 °C (e)–(f). All solid lines indicate the simulated results obtained in this paper by fitting a single exponential component to the simulated TR-OSL curves. These simulated solid lines are compared with the experimental data taken from Figs. 10 and 11 of Ref. [9]. The solid circles in (a) through 6(d) indicate the results obtained in Ref. [9] by fitting the experimental data with a single exponential component. The solid circles and open squares (e) and (f) indicate the results obtained in Ref. [9] by fitting the experimental data with two exponential components. All intensity results were normalized to the initial value at room temperature. The discrepancy at low temperatures between experiment and the model for the 800 °C data in (e) and (f) is due to thermally assisted OSL phenomena which are discussed in the text.

This effect has been interpreted as due to the presence of thermally assisted OSL phenomena (TA-OSL), which are known to influence both the effective luminescence intensity and effective luminescence lifetime [19–21]. TA-OSL effects are empirically described using a thermally assisted OSL activation energy E_{th}. Finally it is noted that the limited model in this paper does not provide a description of the effect of preheating the samples on the TR-OSL signals. In order to describe the effects of preheat on TR-OSL experiments one would use a more comprehensive quartz model, which is outside the scope of this paper.

In summary, the analytical expressions in this paper provide a mathematical description of the variation in quartz of luminescence lifetimes and luminescence intensity with (a) annealing temperature T_{anneal} and (b) with stimulation temperature T. The luminescence lifetimes τ_H and τ_L are associated with recombination processes at two separate centers L_L and L_H, and the annealing process causes a gradual transition of the effective luminescence lifetime from τ_H to τ_L, as the annealing temperature is increased. From a physical point of view, thermal quenching effects are described in the model as competition effects between luminescence and non-luminescencent processes taking place within *each* luminescence center. These competition/thermal quenching processes are consistent with the Mott–Seitz mechanism, and are quantified by two distinct activation energies W_L and W_H, which can be found from the dependence of τ_H and τ_L on the stimulation temperature T. For a compilation of experimental values of energies W_L, W_H, and thermally assisted OSL activation energies E_{th}, the reader is referred to the papers by Chithambo [10,22].

6. The new radioluminescence measurements

Radioluminescence (RL) is the luminescence emitted under exposure of a material to ionizing radiation. For a recent discussion

of the relationship between RL, TL and OSL signals in quartz including an extensive list of references, the reader is referred to the review paper by Preusser et al. [23]. Because the RL signal is measured as a function of the emission wavelength, the method provides a means to study the influence of various experimental parameters on the emission band, including impurities [24], dopants [25] or pre-irradiation annealing [24,26–28]. In this section new experimental results are presented for RL emissions from the same samples which were the subject of the experimental results shown in Figs. 5 and 6 of this paper. Specifically the same commercially available quartz samples (from BDH Ltd., UK) were used in several previous studies [9–13,19,22]. The purpose of the new RL measurements is to investigate whether annealing causes changes in the luminescence bands and their relative intensities in this material, and to assess whether these changes can be correlated with the corresponding effect of annealing on luminescence lifetimes.

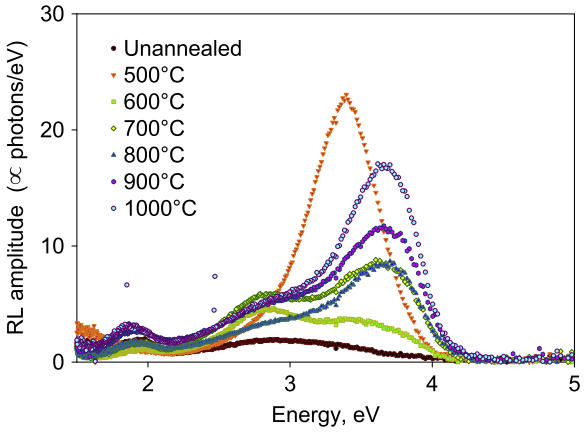

Fig. 7. The RL spectra obtained on the set of commercially available quartz samples, measured at various annealing temperatures. The various emission bands are listed in Table 1. Annealing at 500 °C induces a strong emission band at ~3.44 eV, which decreases significantly for annealing temperatures above 600 °C. Annealing also produces a new emission band at about 3.73 eV, which increases progressively with the annealing temperature.

Radioluminescence measurements were made on a set of quartz samples annealed for 10 min at 500, 600, 700, 800, 900 and 1000 °C and on unannealed samples. The samples were prepared onto stainless steel discs and were X-ray irradiated at a dose rate of 20 Gy min^{-1} using a Philips 2274 X-ray tube, with a Tungsten target, operated at 20 kV/20 mA. The RL signal was recorded using an apparatus reported by Martini et al. [26] featuring a charge coupled device (Jobin-Yvon Spectrum One 3000) coupled to a spectrograph (Jobin-Yvon Triax 180) prepared for signal detection over the range 200–1100 nm. The samples were measured under similar geometric conditions and the uncertainty in the RL signal was determined to be within 10%.

Fig. 7 shows the RL spectra obtained on the set of quartz samples, for various annealing temperatures. The RL spectrum from the unannealed sample in Fig. 7 appears as a combination of at least two broad bands of relatively weak intensity, one near ~2 eV and the other centered at~3 eV. Annealing at 500 °C induces a strong emission band at ~3.42 eV (360 nm), the same one associated with the recombination center involved in the predose effect in TL [26,27,29]. This band decreases significantly when the quartz is annealed at 600 °C and above. Of particular note is that a new emission band appears at about 3.73 eV (330 nm) and is progressively enhanced by annealing temperature, reaching maximum intensity for samples corresponding to annealing temperatures of 1000 °C.

All RL spectra were deconvoluted into their Gaussian components using the Levenberg–Marquardt algorithm, and the results are shown in Figs. 8 and 9. Using previous experience from analysis of emission bands in pegmatitic and synthetic quartz

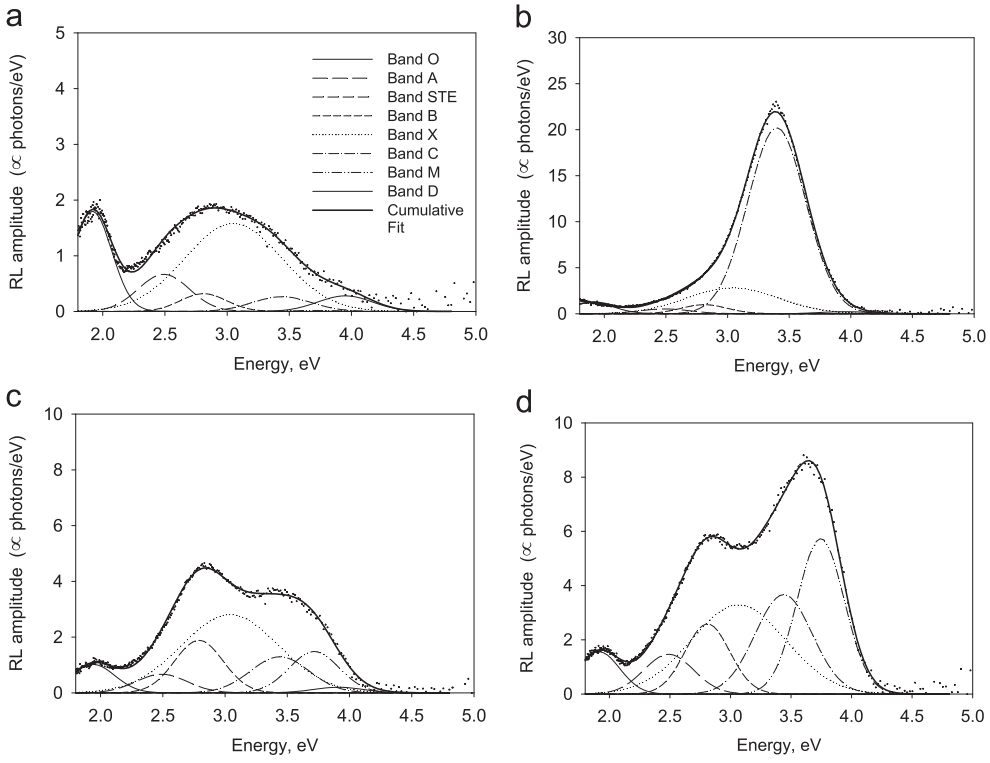

Fig. 8. Deconvolution of RL spectra into their Gaussian components by using a total of 7 emission bands shown in Table 1, and labeled O, A, B, X, C, M and D. Data is shown for unannealed samples and also for quartz annealed at 500, 600 and 700 °C.

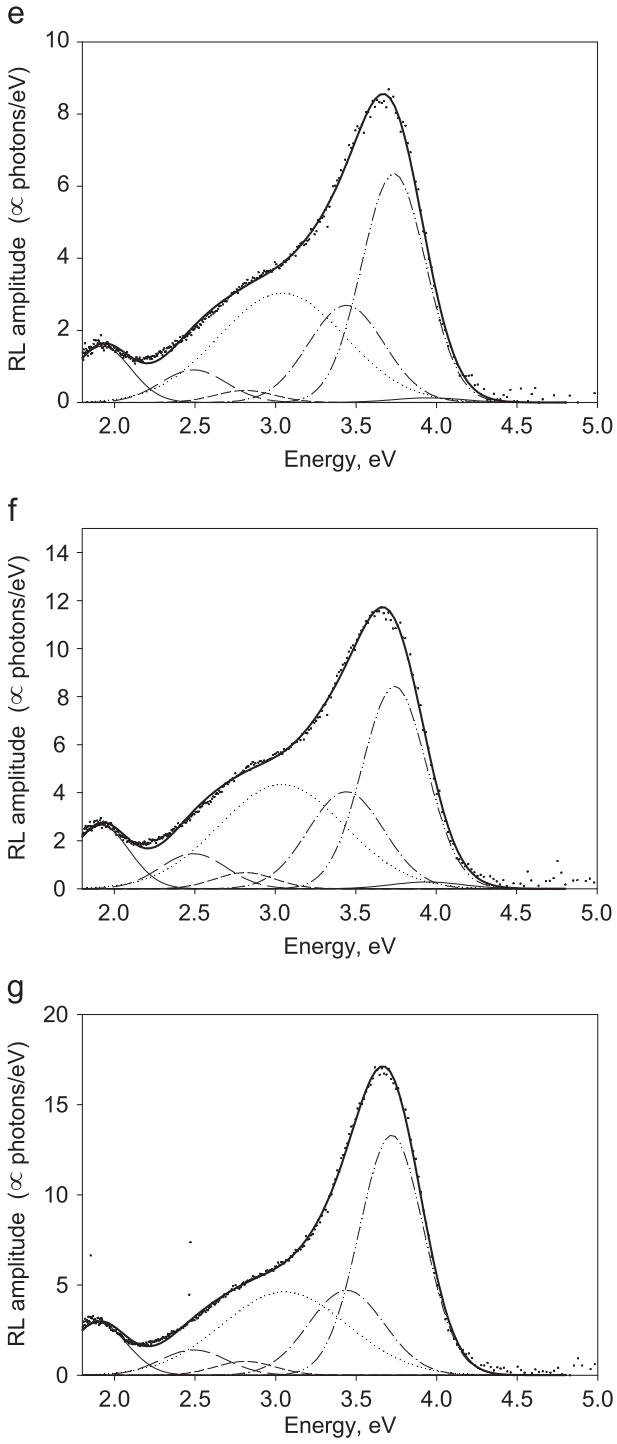

Fig. 9. Same as Fig. 8, for quartz annealed at 800, 900 and 1000 °C

samples [24,26], the fits were initially done using five bands labeled O, A, B, C and D for ease of reference. In further studies, a sixth band was needed to obtain a satisfactory deconvolution and was labeled X [29]. All of these bands are reported in Table 1. In the annealed samples reported in this work, the deconvolution process indicated that using only these six bands could not account for the intense peak around ~3.73 eV (330 nm), and good fits to the emission data required the introduction of a new band with resultant energy ~3.73 eV and FWHM ~0.45 eV. This band is indicated as the M band in Table 1.

Fig. 8 shows the Gaussian fits obtained for quartz annealed at various temperatures. It is evident that band C (3.42 eV, 360 nm) is

Table 1
The wavelength, energy and full width at half maximum for the seven RL emission bands used in the deconvolution of the experimental data shown in Figs. 8 and 9

Band	Wavelength (nm)	Energy (eV)	FWHM (eV)
O	635	1.92	0.39
A	490	2.51	0.46
B	440	2.79	0.46
X	395	3.06	0.89
C	360	3.42	0.58
M	330	3.73	0.45
D	315	3.93	0.49

strongly enhanced by the annealing at 500 °C but is then significantly reduced in intensity when the temperature reaches 600 °C or higher, with the transition apparent around 600–700 °C. However, Band M (3.73 eV, 330 nm) progressively increases in amplitude with annealing temperature. Band B (2.79 eV, 440 nm) is enhanced by annealing at 600 °C (confirming previous results on pegmatitic quartz annealed in different atmospheres), and is quenched when annealed at 800 °C or more. Band X (3.06 eV, 395 nm) is enhanced by annealing at 500 °C but is not significantly affected by annealing at higher temperatures [29].

The thermal dependence of RL emission bands, particularly band C (3.42 eV) and band M (3.73 eV) are consistent with the influence of annealing on luminescence lifetimes in one important respect. The change from the higher lifetime τ_H to the lower one τ_L takes place around 600–700 °C, the same temperature region where the change in the importance of RL emission from band C (3.42 eV) to band M (3.73 eV) becomes apparent. As discussed previously, this feature reflects the change in dominance of luminescence emission, from the L_H to the L_L centers. This is evident in Figs. 7 and 8. In fact, the behavior of the M band (~3.73 eV) shows a qualitative correlation with the hypothesized behavior of the L_L center in the model.

The unambiguous identification of certain radioluminescence bands with specific defects in order to identify the recombination centers L_H and L_L is not straightforward. An important question in comparing the TR-OSL and RL experimental data is whether the RL emission-bands are identical to the bands detected during OSL experiments. Indeed there is no direct experimental proof that the two sets of emission bands are the same.

For one thing, excitation is clearly different in the RL and TR-OSL processes, since the former is observed under continuous X-ray irradiation, whereas the TR-OSL signal is detected under optical excitation and only after the sample has been irradiated. It is likely that the emission centers as well as the source of the electrons for the RL and TR-OSL processes are different. Nevertheless, some observations and propositions can be made on the basis of extensive previous experimental work on quartz [23]. It is known that irradiation above 200 K dissociates alkali ions (M^+) from [AlO_4/M^+] centers, leading to formation of [AlO_4/H^+]^0 and [AlO4]^0. Heating the quartz samples above 300 °C causes the alkali ions to return to the Al sites, hence restoring the material to its pre-irradiation state [23]. However, this view might be an oversimplification, since the heating process may return alkali ions to AlO_4 sites, but not necessarily to the newly generated [AlO_4/H^+]^0 sites. As a consequence, the sample conditions after heating may not necessarily be the same as before heating.

In general terms, the increase in photon emission associated with certain RL bands after annealing, can be interpreted as reflecting an increase in the concentration of recombination centers. However, this may not be the only explanation of the sensitization effect observed in quartz. For example, it has been argued that this increase in photon emission may be due to a decrease of competition centers such as the E' center, as was shown in the comprehensive work by Schilles et al. [30].

7. Discussion

In this section we summarize the results of several recent experimental studies, and their relevance to the RL data presented in the previous section. The luminescence process in quartz is known to be extremely complex, and several experimental studies have attempted to correlate specific defects with the experimentally observed luminescence emission in this material. It is generally accepted that there are multiple types of luminescence centers in quartz, and that some of these centers are dominant depending on the experimental treatments such as irradiation, annealing and measurement temperatures, or on some combination of these parameters. The lifetime features discussed in the purposefully annealed quartz are also observed in natural quartz corresponding to various thermal provenances [31]. It was previously reported for example that lifetimes in metamorphic quartz with a provenance temperature of 450–550 °C comprised only of the longer L_H component, whereas in plutonic quartz with a corresponding thermal provenance of 550–700 °C only the shorter component was found [31]. Meanwhile, the non-radiative recombination center R is insensitive to sunlight bleaching and for this reason the predose dating technique (which is based on the behavior of the center R) can be applied to materials which have been exposed to sunlight [16].

Preusser et al. [23] pointed out the complexity of the luminescence process and discussed the effects due to intrinsic defects in quartz (such as Si and O vacancies), as well as effects due to common quartz impurity atoms (like Al or Ti). Furthermore, they emphasized the importance of alkali ions in the luminescence process in quartz, and reviewed the various models in the literature. The current consensus for the various electronic and ionic processes involved in TL and OSL of quartz was summarized in Preusser et al. [23], their Table II.

Recently Martini et al. [24] studied the RL signals of synthetic quartz samples in which the concentrations of alkali ions were changed by electrodiffusion treatments. The RL spectra were found to be composed of a total of four bands. The well known blue emission at around 470 nm was found to be a composite of a 430 nm (2.86 eV) band and of a second band at 485 nm (2.53 eV). The authors labeled the 485 and 430 nm bands as A and B bands, with the A band being the most intense in the untreated and Li-swept samples. In untreated samples an additional intense UV emission was found at 315 nm (3.94 eV) and was labeled the D band. These authors reported an increase, under irradiation, of the 485 nm band intensity and a decrease in the 430 nm emission in the Li swept-in samples. The previously reported C band (355 nm, 3.44 eV) UV emission was detected for all the samples, and was the most intense in their swept out samples. The authors attempted possible assignments of the detected emission bands as related to specific defects and impurities in quartz, such as the Al centers which are most affected by sweeping procedures. Martini et al. [24] proposed that the behavior of the A band is related to Li^+ ions and specifically to $[AlO_4/Li^+]$ centers known to be present in quartz. Furthermore, it was suggested that the B band may be related to an OH and/or Na^+ center involving Al ions, with $[AlO_4/H^+]^\circ$ and $[AlO_4/Na^+]^\circ$ centers being the possible candidates. The authors noted that the C emission band was reported in older studies as either 365 nm or as 380 nm, and was previously assigned to the $[AlO_4]^\circ$ center [32,33], or alternatively to $[H_3O_4]$ centers [34] based on ESR studies. Martini et al. [24] also suggested that the D band emission may be correlated with oxygen vacancies in quartz.

In a companion study Martini et al. [26] studied the effect of X-ray irradiation and thermal treatments on the RL signal from a natural pegmatitic and a synthetic quartz sample. The emission spectra from these samples were deconvoluted using five Gaussian components. A series of irradiation followed by heating of the samples to 500 °C caused strong sensitization of both the C band (3.44 eV) and of the well known 110 °C TL peak. In addition, X-ray irradiation was found to enhance the 2.53 eV (480 nm) emission and a strong correlation was also found between this emission and the sensitivity of the 110 °C TL peak. Therefore both these bands are believed to participate in both RL and TL luminescence mechanisms..

In another notable recent study, King et al. [35] studied a suite of quartz samples of different provenances and geological histories using spectroscopic ionoluminescence (IL) to investigate variations in emission spectra as a function of radiation dosing. Specifically these authors studied variations in the UV-violet emission (3.2–3.4 eV) and also in the red emission (1.8–1.9 eV) with increasing cumulative dose. These authors examined the emission at different doses, and concluded that the overall reduction in the UV-violet emission at 380 nm (~3.3 eV) is caused by reductions in the populations of $[AlO_4/M^+]^\circ$ and $[AlO_4]^\circ$ type centers. Their experiments showed that these population changes are caused by ion and electron migration, and their data were consistent with a mechanism in which ion and electron migration causes a change in the center types according to the processes:

$$[AlO_4/M^+]^0 \gg [AlO_4/h^+]^0 + M^+(\text{free}) \gg [AlO_4]^- + \text{NBOHC (free)}$$

$$\text{Luminescence}: \quad 3.3\ \text{eV} \quad 3.6\ \text{eV} \qquad\qquad 1.9\ \text{eV}$$

where NBOHC denotes a paramagnetic non-bridging oxygen hole center, a well-known defect in quartz. Furthermore, King et al. [35] discussed the correlation between the thermal and irradiation history of quartz samples and their OSL luminescence efficiency. They suggested that recently eroded quartz samples have poor luminescence sensitivity due to their immediate geological irradiation history. On the contrary, highly weathered quartz has probably undergone many cycles of deposition and transport, and will have been exposed to high temperatures or mechanical processes during transport. These processes will have allowed remigration of the alkali ions to their charge compensating interstitial locations, resulting in $[AlO_4/M^+]^\circ$ center formation, and therefore result in a high efficiency of the UV-blue emissions. One would then expect such well weathered samples to have good OSL properties.

8. Conclusions

This paper presented an analytical model for thermal quenching in quartz, which includes two distinct luminescence centers L_H and L_L and a hole reservoir R. Analytical expressions are obtained for the intensity of light during a TR-OSL experiment, and are shown to be in agreement with published experimental data for commercially available quartz samples. The model describes two different thermal effects in quartz, namely the variation of the luminescence lifetimes with (a) annealing temperature and (b) stimulation temperature. The modeling results were supplemented by new RL measurements carried out using the same annealed quartz samples, and Gaussian deconvolution showed the presence of seven RL emission bands. The behavior of the M band at ~3.73 eV was found to be qualitatively correlated with the hypothesized behavior of the concentrations of holes N_L in the model.

The promising preliminary RL results shown in Figs. 7 and 8 indicate that it should be possible, at least in principle, to correlate the experimental behavior of luminescence lifetimes in annealed quartz samples with the emissions from specific recombination centers. Clearly more experimental and modeling work is necessary to provide a better description of the luminescence process in quartz, and to explain possible correlations between different types of experimental results.

Acknowledgments

We acknowledge with gratitude financial support for the 2012 International Symposium on Luminescence held in Port Elizabeth, South Africa and funding for the Italy/South Africa Research Cooperation Programme (National Research Foundation, South Africa; KFD Development Grant and UID 74341) both of which were helpful in part in bringing the work reported here to completion.

References

[1] D.C.W. Sanderson, R.J. Clark, Radiat. Meas. 23 (1994) 633.
[2] I.K. Bailiff, Radiat. Meas. 32 (2000) 401.
[3] S. Tsukamoto, P.M. Denby, A.S. Murray, L. Bøtter-Jensen, Radiat. Meas. 41 (2006) 779.
[4] P.M. Denby, L. Bøtter-Jensen, A.S. Murray, K.J. Thomsen, P. Moska, Radiat. Meas. 41 (2006) 774.
[5] M.L. Chithambo, F.O. Ogundare, J. Feathers, Radiat. Meas. 43 (2008) 1.
[6] C. Ankjærgaard, M. Jain, R. Kalchgruber, T. Lapp, D Klein, S.W.S. McKeever, A. S Murray, P. Morthekai, Radiat. Meas. 44 (2009) 576.
[7] V. Pagonis, S.M. Mian, M.L. Chithambo, E. Christensen, C.J. Barnold, J. Phys. D: Appl. Phys. 42 (2009) 055407.
[8] C. Ankjærgaard, M. Jain, K.J. Thomsen, A.S Murray, Radiat. Meas. 45 (2010) 778.
[9] R.B. Galloway, Radiat. Meas. 35 (2002) 67.
[10] M.L. Chithambo, Radiat. Meas. 37 (2003) 167.
[11] M.L. Chithambo, Radiat. Meas. 41 (2006) 862.
[12] M.L. Chithambo, J. Phys. D: Appl. Phys. 40 (2007) 1874.
[13] M.L. Chithambo, J. Phys. D: Appl. Phys. 40 (2007) 1880.
[14] B.W. Smith, E.J. Rhodes, S. Stokes, N.A. Spooner, Radiat. Prot. Dosim. 34 (1990) 75.
[15] N.A. Spooner, Radiat. Meas. 23 (1994) 593.
[16] L. Bøtter-Jensen, S.W.S. McKeever, A.G. Wintle, Optically Stimulated Luminescence DosimetryElsevier, Amsterdam, 2003.
[17] R. Chen, V. Pagonis, Thermally and Optically Stimulated Luminescence: A Simulation Approach, Wiley and Sons, Chichester, 2011.
[18] R.M. Bailey, Radiat. Meas. 33 (2001) 17.
[19] M.L. Chithambo, R.B. Galloway, Nucl. Instrum. Methods Phys. Res. B 183 (2001) 358.
[20] V. Pagonis, C. Ankjærgaard, A.S. Murray, R. Chen, J. Lumin. 130 (2010) 902.
[21] V. Pagonis, J. Lawless, R. Chen, M.L. Chithambo, J. Lumin. 131 (2011) 1827.
[22] M.L. Chithambo, F.O. Ogundare, Radiat. Meas. 44 (2009) 453.
[23] F. Preusser, M.L. Chithambo, T. Götte, M. Martini, K. Ramseyer, E.J. Sendezera, G.J. Susino, A.G. Wintle, Earth-Sci. Rev. 97 (2009) 196.
[24] M. Martini, M. Fasoli, A. Galli, I. Villa, P. Guibert, J. Lumin. 132 (2012) 1030.
[25] M.L. Chithambo, S.G. Raymond, T. Calderon, P.D Townsend, J. Afr. Earth Sci. 20 (1995) 53.
[26] M. Martini, M. Fasoli, I. Villa, P. Guibert, Radiat. Meas. 47 (2012) 846.
[27] J. Zimmerman, J. Phys. C 4 (1971) 3265.
[28] S.W.S. McKeever, J.A. Strain, P.D. Townsend, R.A. Wood, Eur. PACT J. 9 (1983) 123.
[29] M. Martini, Private Communication, 2013.
[30] T. Schilles, N.R.J. Poolton, E. Bulur, L. Bøtter-Jensen, A.S. Murray, G.M. Smith, P.C. Riedi, G.A. Wagner, J. Phys. D: Appl. Phys. 34 (2001) 722.
[31] M.L. Chithambo, F. Preusser, K. Ramseyer, F.O. Ogundare, Radiat. Meas. 42 (2007) 205.
[32] M. Martini, A. Paleari, G. Spinolo, A. Vedda, Phys. Rev. B 52 (1995) 138.
[33] J. Gotze, M. Plotze, T. Trautmann, Am. Mineral. 90 (2005) 13.
[34] X.H. Yang, S.W.S. McKeever, Radiat. Prot. Dosim. 33 (1990) 27.
[35] G.E. King, A.A. Finch, R.A.J. Robinson, D.E. Hole, Radiat. Meas. 46 (2011) 1.